



High Pressure Resistant Aramid Fiber Reinforced Polymer Matrix Composite Pipe Design

Yüksek Basınca Dayanıklı Aramid Elyaf Takviyeli Polimer Matris Kompozit Boru Tasarımı

Ali Ari^{1*} and Ali Bayram²

¹Vocational School of Weapon Industry Technician Department, OSTİM Technical University, Ankara, Turkey.

²Faculty of Engineering, Department of Mechanical Engineering, Bursa Uludağ University, Bursa, Turkey.

ABSTRACT

In this study, a total of 6 different composites were obtained by adding 5%, 10% and 15% chopped aramid fiber reinforcement in 6 mm dimensions to each of the polypropylene and polyethylene matrix elements under the same production method and same conditions. The reinforcement and matrix materials were mixed using the extrusion method and then formed into plates by the press molding technique. The mechanical properties of these composites were investigated by performing tensile and charpy tests, and the effects of the surface energy of the matrix on the composite were discussed. S/N ratios were calculated for the mechanical properties of the composites and the effect of the matrix, fiber and additive ratios on mechanical properties was determined using analysis of variance (ANOVA). According to the Signal/Noise (S/N) ratios and ANOVA results, it was observed that the composites had different effects on the mechanical properties. Pipes are designed considering the mechanical properties of composite materials with 15% aramid fiber added to each matrix element. The composite pipe design to be pressure tested was designed in Solidworks program with a length of 500 mm according to ISO 1167 standards. Pipe dimensions with an outer diameter of 125mm, which are used as a standard in natural gas infrastructure works, are taken as reference.

Key Words

Chopped fiber, polypropylene, polyethylene, ANOVA, pipe.

Öz

Bu çalışmada, polipropilen ve polietilen matris elemanlarının her birine aynı üretim yöntemi ve aynı koşullarda 6 mm boyutlarında %5, %10 ve %15 kırılmış aramid elyaf takviyesi eklenerek toplam 6 farklı kompozit elde edilmiştir. Takviye ve matris malzemeleri ekstrüzyon yöntemiyle karıştırılmış ve daha sonra pres kalıplama tekniği ile plakalar haline getirilmiştir. Bu kompozitlerin çekme ve charpy testleri yapılarak mekanik özellikleri incelenmiş ve matrisin viskozite ve yüzey enerjisinin kompozit üzerinde etkisi tartışılmıştır. Kompozitlerin mekanik özellikleri için S/N oranları hesaplanmış ve matris, elyaf ve katkı oranlarının mekanik özelliklere etkisi varyans analizi (ANOVA) kullanılarak belirlenmiştir. Sinyal/Gürültü (S/N) oranları ve ANOVA sonuçlarına göre kompozitlerin mekanik özellikler üzerinde farklı etkileri olduğu gözlemlenmiştir. Borular, her matris elemanına %15 aramid elyaf ilave edilerek kompozit malzemelerin mekanik özellikleri dikkate alınarak tasarlanmıştır. Basınç testi yapılacak kompozit boru tasarımı, ISO 1167 standartlarına göre 500 mm uzunluğunda Solidworks programında tasarlanmıştır. Doğalgaz altyapı işlerinde standart olarak kullanılan 125mm dış çaplı boru ölçüleri referans alınmıştır.

Anahtar Kelimeler

Kırılmış fiber, polypropylene, polyethylene, ANOVA, boru.

Article History: Received: Dec 7, 2021; Revised: Mar 10, 2022; Accepted: Mar 10, 2022; Available Online: Jul 5, 2022.

DOI: <https://doi.org/10.15671/hjbc.1024810>

Correspondence to: A. Ari, Vocational School of Weapon Industry Technician Department, OSTİM Technical University, Ankara, Turkey.

E-Mail: ali.ari@ostimteknik.edu.tr

INTRODUCTION

Short fiber reinforced polymers (SFRP) are becoming increasingly popular in various application areas such as the automotive and construction industries [1]. High-performance materials are obtained by combining polymers with the advantages of good impact resistance and low weight with the high stiffness and strength of reinforcing fibers [2]. In addition, many chopped fiber reinforced polymers are suitable for mass production as conventional techniques such as extrusion and injection molding can be used [3]. Traditional reinforcing fibers are usually glass fibers because it offers good strength and stiffness, impact resistance, chemical resistance, and thermal stability at a low price [4]. However, since glass fiber is not sufficient for special applications, it is necessary to use other fiber types. For example, carbon fiber is used when high stiffness is required [5], while aramid fiber shows high impact resistance [6].

Glass fiber is constantly used in the manufacture of pipes that require high pressure and high temperature [7]. Polypropylene composites reinforced with continuous glass fibers have a higher modulus of elasticity than pure polypropylene due to the stiffening effect of the fibers [8]. However, continuous glass fibers limit the processing and forming capabilities of composites. The injection method is common in the production of randomly oriented long (ranging from 5 to 25 mm) and short (less than 3 mm) fiber-reinforced composites [9]. This method provides flexibility and significant strength values in the production of short glass fiber reinforced composites [10]. Therefore, polymer composites reinforced with chopped fibers are used in pipe production. However, polymer reinforcement fails when the fiber length is less than the critical length required to transfer the mechanical load from the polymer matrix to the

fiber [11]. It also exhibits undesirable performance due to its high fiber content, poor fiber-matrix interaction, widening of matrix cracks and consequent low load bearing capacity [12].

Recently, aramid fiber reinforced polymer composites have been highly preferred. It has been preferred in engineering fields due to its high strength values and low densities [13]. Various studies have been carried out to modify the aramid fiber surface in order to improve the interfacial adhesion between the fiber and the matrix. The purpose of aramid fiber surface modification is to improve the chemical activity of the surface, increase the surface roughness and provide an excellent chemical bond and mechanical interlocking between the fiber and the matrix [14].

In the study, polypropylene (PP), and polyethylene (PE), were chosen as matrix materials and the matrix materials were reinforced with aramid fibers. The main objective of this study is to provide detailed and collective information about the mechanical properties of the composites in question since the above-mentioned composites have a wide area of use in engineering applications and contribute to the literature.

MATERIALS and METHODS

Material and Production Method

In the experimental studies, PP and PE were used as matrix materials and aramid (Twaron) fibers were used as reinforcement material. Chopped fiber of 6 mm length was used in composites. The fiber ratios were determined as 5%, 10% and 15%. The mechanical properties of matrix and fiber materials are taken from the catalog values (Table 1).

Table 1. Mechanical properties of materials.

Materials	Density (g/cm ³)	Tensile Strength (MPa)	Stress Modulus (GPa)	Elongation at Break (%)
Polypropylene (PP)	0.9	38	1.3	> 50
Polyethylene (PE)	0.95	24	1.1	> 50
Aramid Fiber (AF)	1.44	2800	70	2.3-4.2

Twin screw extruder (Polmak Plastik 22 mm Lab type research extruder) was used for composite production. The temperature values for the five zones in the extruder were determined using the literature and the product catalog of the materials (Table 2). After the composites were obtained, they were granulated with a cutter. 500mmx500mm composite plates were obtained by granular press molding method. The production parameters of composites made with each matrix are shown in figure 1. Molding consists of 3 stages and all samples taken were kept for 120 seconds in the first

stage, 180 seconds in the second stage and 60 seconds in the third stage. The test samples were prepared by cutting the relevant molds in standard dimensions on the CNC machine [15,16].

Experimental Design and Anova Analysis

In this study, it is necessary to determine the experimental factors and their levels to interpret their effects on the response variable by making the changes in Table 3 [17].

Table 2. Extrusion production parameters.

Matrix Material	Extruder Temperature	Screw Rotation Speed (rpm)
Polypropylene	195-215-225-225-240	30
Polyethylene	170-195-220-220-230	30

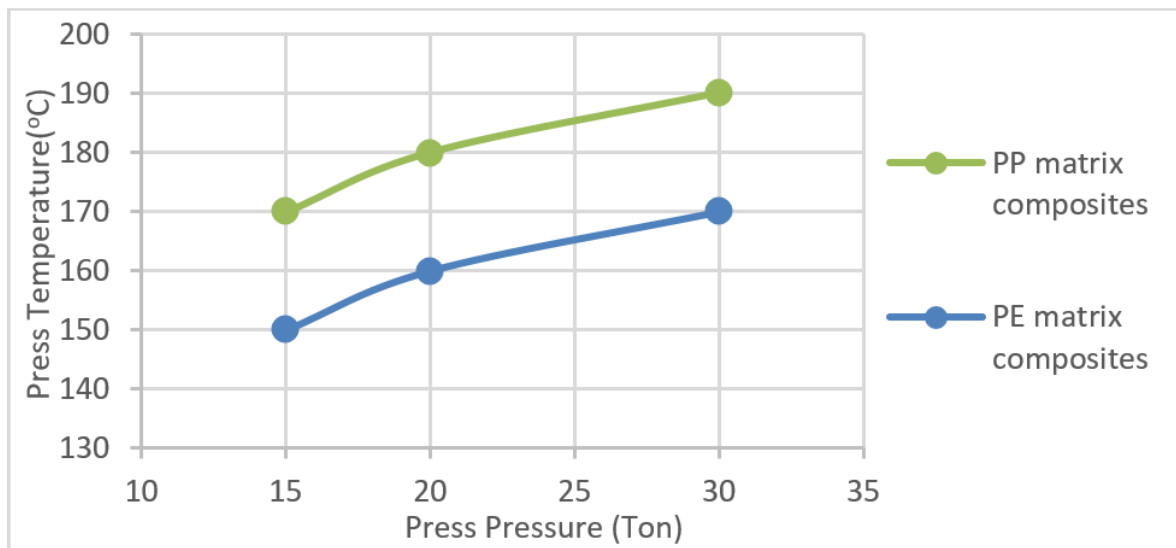


Figure 1. Press molding production parameters.

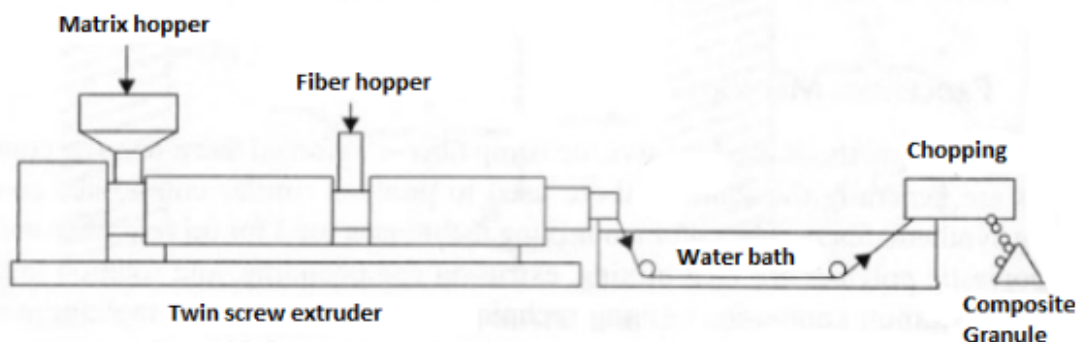


Figure 2. Chopped fiber production in twin screw extruder.

Table 3. Experiment factors and levels.

Factors	1. Level	2. Level	3. Level	4. Level
A- Matrix Type	PP	PE	-	-
B- Fiber Percentage %	0*	5	10	15

Table 4. Experimental design.

Experiment No	A-Matrix Type	B-Fiber Percentage %
1	1	1
2	2	1
3	1	2
4	1	3
5	1	4
6	2	2
7	2	3
8	2	4

In this process, the experimental matrix indicated in Table 4 was used to observe, obtain and interpret the effects on the response variable by making desired changes on the input variables [18].

In the analysis of variance, it is revealed to what extent the examined factors affect the output value chosen to measure quality and how kind of variability different levels cause. In addition, the statistical reliability of the obtained results is also tested. For this purpose, first of all, the SST value (sum of total squares), which indicates the total variability of the signal/noise (S/N) ratio, is calculated according to equation 1 [19].

$$SS_T = \sum_{i=1}^n (\eta_i - \eta_m)^2 \quad (1)$$

In Equation 1, η_i is the signal-to-noise ratio calculated over the measured value, η_m is the average of the signal-to-noise ratios calculated over the measured value, and n is the total number of experiments [20]. The SST value consists of the sum of the squares of the three factors (SSA, SSB, and SSC) and the SSE value is the sum of the squares of the margin of error. The sum of the squares of each factor was calculated separately using equation 2.

$$SS_A = \sum_{i=1}^{k_A} [n_{A_i} x (\eta_{A_i} - \eta_m)^2] \quad (2)$$

In Equation 2, k_A represents the number of levels of the A factor, the number of experiments at the i level of the A factor, the S/N ratio of the A factor at the i level, and the average S/N ratio.

Then the F-Test is performed by calculating with equation 3 to show how much each experimental factor affects the test results.

$$F = \frac{SS_A/k - 1}{SS_E/N - k} \quad (3)$$

In Equation 3, $k-1$ is the degree of freedom for the numerator by subtracting one from the number of groups, $N-k$, the degree of freedom for the denominator is determined by subtracting the number of groups from the number of observations in all groups [21].

RESULTS and DISCUSSION

Tensile Properties and Fractography

Tensile tests were completed with the Besmak-BMT 100E brand Universal Tensile Tester (100 kN). Tensile test specimens were prepared according to TS EN ISO 527-2 type 2 standards. Tensile speed was set to 2 mm/min, and pre-tension value was set to 10N. The measuring length is 50 mm video extensometer. Test conditions completed at 21 °C. Fractured surface images of 15% fiber reinforced samples were examined with Hitachi TM3000 brand SEM.

It was observed that as the ratio of AF increased, the tensile strength of the composites increased and the highest tensile strength was observed in the reinforced composites with 15%. When the matrix materials were compared, it was seen that the best performance was 15% AF reinforced PE composite.

-15% AF increased the tensile strength of PE by 1.7 times and increased it from 19 MPa to 34 MPa.

-15% AF increased the tensile strength of PP by 1.5 times and increased it from 38 MPa to 57 MPa.

The yield of fibers on matrix materials can be calculated using the Kelly–Tyson model [22].

$$\sigma_c = \lambda_f \sigma_f V_f + \sigma_m (1 - V_f) \quad (4)$$

The yield decreased gradually with the increasing fiber content of PP. However, as the PE fiber ratio increased, the yield increased, but after 15%, the graph started to draw a horizontal direction. This means that the PE+15% AF mixture is optimal. When we look at the literature, the fiber yield is expected to be between 0.2-0.38 in the form of randomly dispersed fibers in the matrix [23]. In our study, the fiber yield of 15% AF reinforced PE was 0.03, and the fiber yield of 15% AF reinforced PP was 0.06. This showed us the result that the bond formation between the fiber and the matrix is weak [24].

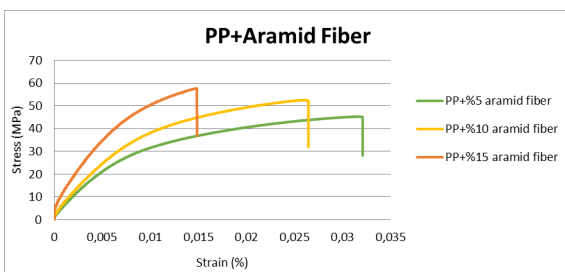


Figure 3. Tensile test results of PP+AF composites.

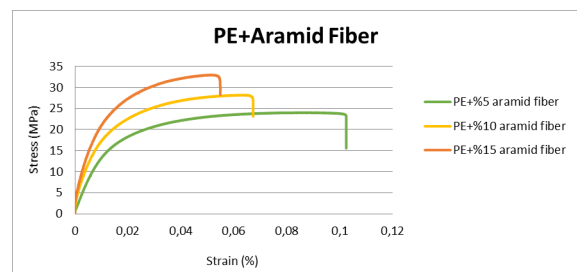


Figure 4. Tensile test results of PE+AF composites.

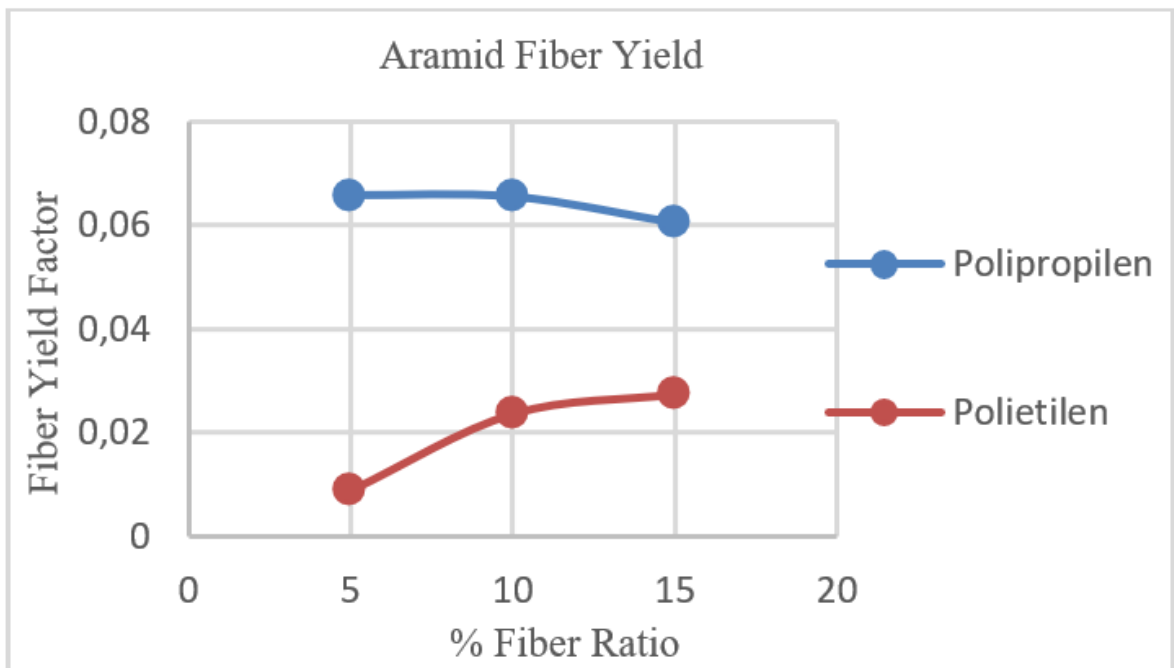


Figure 5. Aramid fiber yield factor in PP and PE.

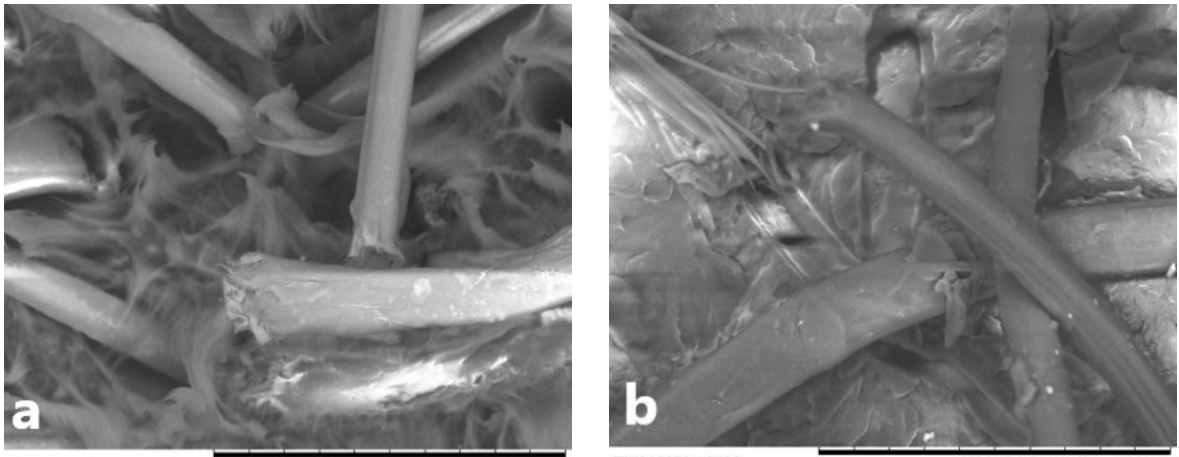


Figure 6. SEM images of 15% AF reinforced a) PE and b) PP composites aramid fiber reinforced.

Figure 6 shows SEM images of 15% fiber reinforced composites. It is seen that there is pull out in the fibers and when the surface of the fibers is examined, it is not covered with a polymeric matrix. This indicates poor interface adhesion between fiber and matrix. Dark circles around the fibers indicate local deformation of the matrix around the fibers. In addition, these dark circles at the interface indicate that the fibers are not connected

with the matrix. The dark circle is caused by local deformation of the matrix around the fiber after the fibers are separated from the matrix. When the fracture surfaces of the 15% AF reinforced composites were examined, it was observed that bending and crossing occurred in the fibers with the increase in the fiber content. This adversely affected fiber performance [25].

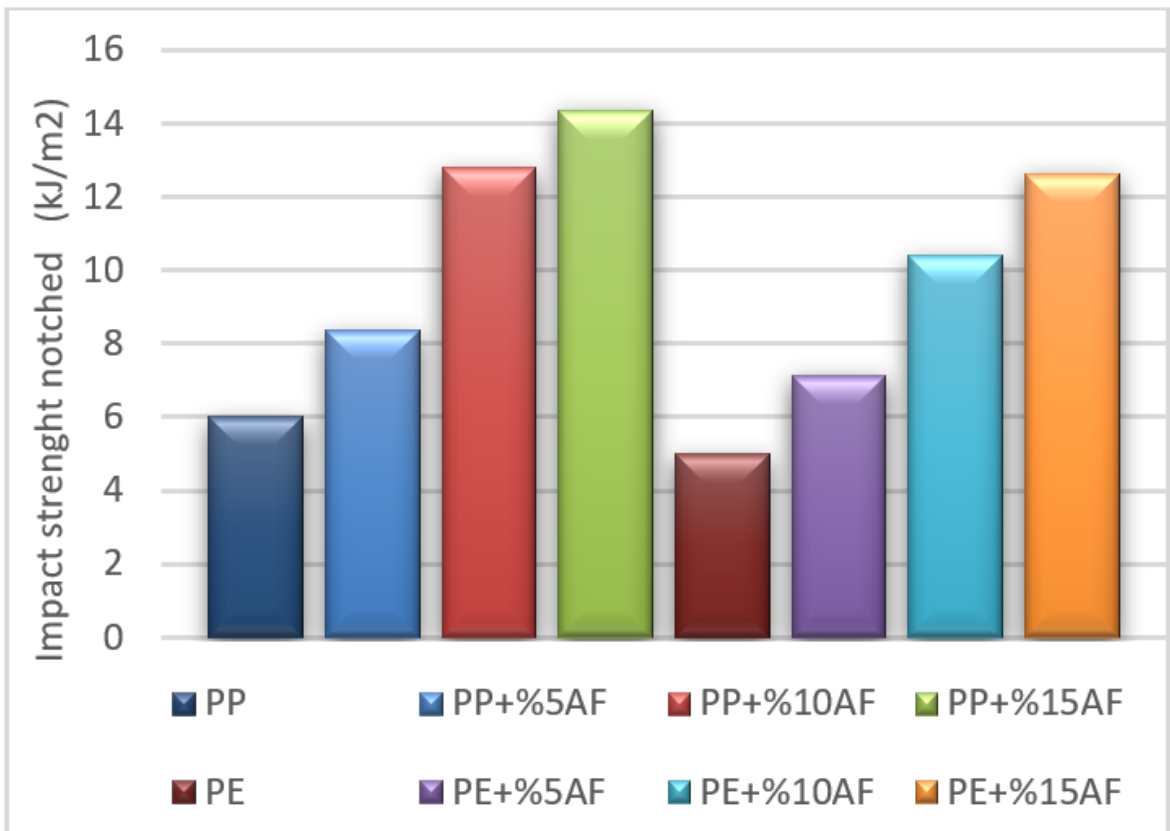


Figure 5. Aramid fiber yield factor in PP and PE.

Charpy impact Properties

Experiments were made in Testform-SDTC-50J/PL-057 brand impact tester. Charpy impact test specimens were prepared with notches according to TS EN ISO 179-1 standards and the tested ambient temperature was set as 21 °C.

When the impact results of the composites are examined (figure 7.), it is seen that the impact force increases as the fiber ratio increases. However, Aramid Fiber showed higher performance with PP matrix composite.

-15% AF increased the tensile strength of PE by 2,6 times and increased it from 5 MPa to 13 MPa.

-15% AF increased the tensile strength of PP by 2.38 times and increased it from 6 MPa to 14.3 MPa.

Analysis of Experimental Results

Signal value (S) denotes the actual value presented by the system and intended to be measured. The noise factor (N) refers to the share of undesirable factors in the measured value. The aim of this study is to reach the highest value. The equation below is used to calculate the S/N ratio according to this method [26]. S/N ratios of test results are shown in Table 4.

$$S/N = -10 \log_{10} \left[\frac{1}{n} \sum_{i=1}^n y_i^2 \right] \quad (5)$$

In Equation 5, y_i is the measurement value and n is the number of experiments.

Table 5. S/N ratios of experimental results.

Experiment No	Tensile (MPa)	S/N	Charpy impact (kJ/m2)	S/N
1	38	31.59	6	15.56
2	19	25.57	5	13.97
3	45.32	33.12	8.35	18.43
4	52.56	34.41	12.78	22.13
5	57.73	35.22	14.35	23.13
6	24.04	27.61	7,3	17.06
7	28.22	29.01114	57.41	35.18
8	31.92	30.081258	42.9142	32.65

For the next section, the impact of each factor at each level should be disassembled. For this purpose, the average of the S/N ratios calculated in Table 5 is considered independent for each level of each factor. The greatest signal-to-noise ratio gives the best experimental result. These values are graphically presented in Figures 8-9. The highest S/N ratio was the PP in all tests. Meanwhile, the S/N ratio increases as the fiber percentage increases. It is seen that the composites are quite effective on the tensile strength of the marix type.

When the S/N ratios of the tensile and charpy tests are examined (Figure 8-9), it is seen that the mechanical properties increase as the fiber ratio increases. In addition, molecules in a low surface energy liquid are not strongly attracted to each other; instead, they tend to spread and adhere to the surface, so a high free energy liquid will not bind to the fiber surface. To form a good bond, the matrix surface energy must be low [27]. Since the surface energy of the PP matrix is lower than that of the PE matrix, the composite with PP matrix performed better [28].

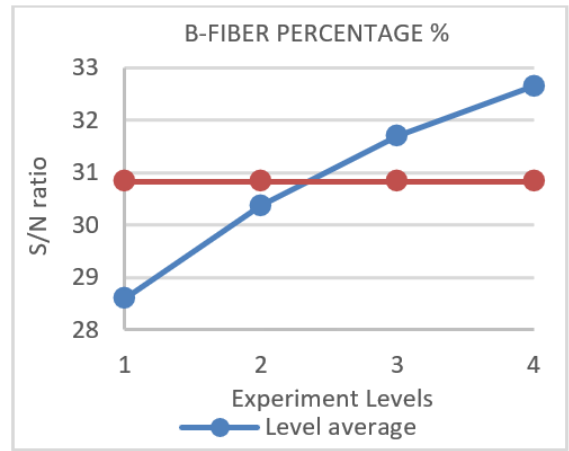
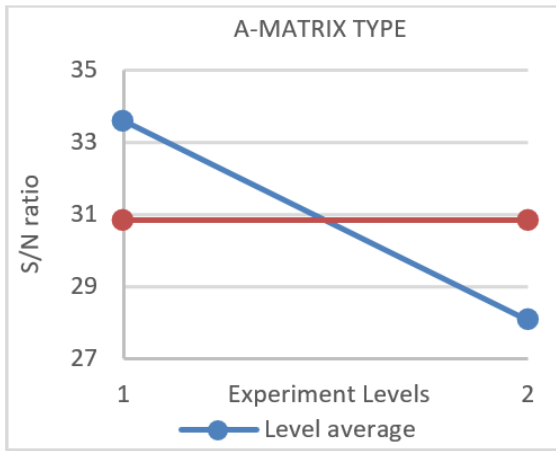


Figure 8. S/N Ratios for Tensile Strength.

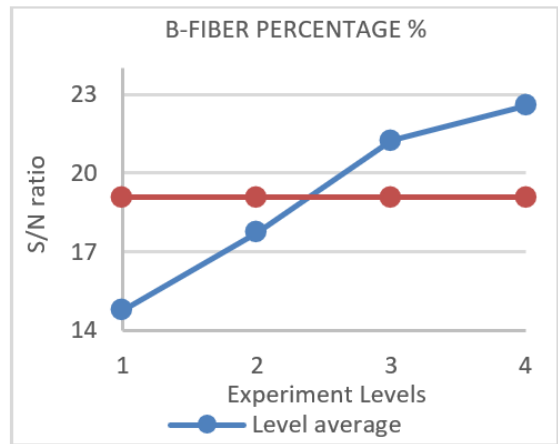
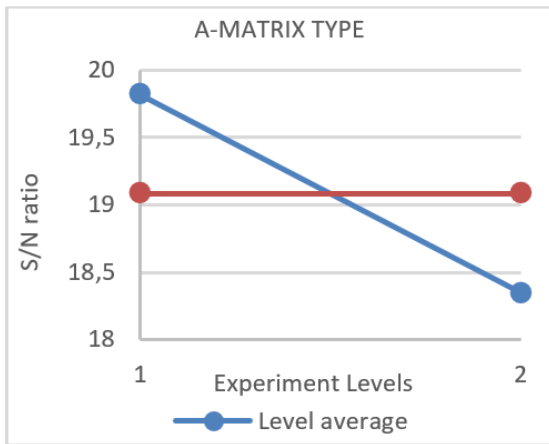


Figure 9. S/N Ratios for Charpy Test.

Table 6. ANOVA Table for Tensile Test.

S/N ratio: 30,83		Average S/N Values							
	Degrees of Freedom	Level 1	Level 2	Level 3	Level 4	Sum of Squares	Variance	F	Percentage of Contribution (%)
A- MATRIX TYPE	1	33.59	28.07	0.00	0.00	60.92	60.92	603.19	90.58
B- FIBER PERCENTAGE %	3	28.59	30.37	31.71	32.65	18.71	6.24	61.75	9.27
Error	2					0.20	0.10		0.15
Total	6					79.83	67.26		

Table 7. ANOVA Table for Charpy Test.

S/N ratio: 19,08		Average S/N Values							
	Degrees of Freedom	Level 1	Level 2	Level 3	Level 4	Sum of Squares	Variance	F	Percentage of Contribution (%)
A- MATRIX TYPE	1	19.82	18.35	0.00	0.00	4.30	4.30	65.95	14.72
B- FIBER PERCENTAGE %	3	14.77	17.75	21.23	22.58	74.47	24.82	381.07	85.06
Error	2					0.13	0.07		0.22
Total	6					78.90	29.19		

	Degrees of Freedom	Level 1	Level 2	Level 3	Level 4	Sum of Squares	Variance	F	Percentage of Contribution (%)
A- MATRIX TYPE	1	19.82	18.35	0.00	0.00	4.30	4.30	98.93	14.73
B- FIBER PERCENTAGE %	3	14.77	17.75	21.23	22.58	74.47	24.82	571.60	85.12
Error	3					0.13	0.04		0.15
Total	7					78.90	29.16		

To explain how each experimental factor influences the experimental results, the calculated F values are 1 for the A factor, 3 for the B factor and 3 for the error term, the degrees of freedom taken from the critical F table are F 0.05;1;2 (18.53) and F are compared with 0.05;3;2 (19.164). The calculated F values were greater than the critical F values and provided the targeted 95% confidence level.

When Table 6-7 is examined, it is seen that the factor affecting the tensile strength of composite materials the most is the matrix type with 90.58%. It was observed that the factor affecting the impact resistance the most was the fiber additive ratios with 85.06%. It was observed that the effect on the matrix material increased as the fiber additive ratio increased [29].

Finite Element Analysis of Composite Pipes

Numerical finite element analysis ANSYS program 2021 R1 version was used in the pressure test of composite materials in the computer environment. The mechanical properties of the materials are taken from the test results.

If we list the steps of problem definition in ANSYS in its most basic form,

- Material Identification
- 3D Model Creation
- Creating Mesh
- Definition of Boundary Conditions
- Problem Solving
- Results

Material Identification

When the test results are examined, it has been seen that the increased fiber ratio improves the mechanical properties of the materials. Therefore, pipes are designed considering the mechanical properties of composite materials with 15% fiber added to each matrix element.

When the material densities are calculated theoretically;

The fiber volume ratio is defined as V_f , the matrix volume ratio V_m and their density ρ . Accordingly, the theoretical density calculation of composite materials can be made from the following equation 6.

$$\rho_c = \rho_f V_f + \rho_m V_m \tag{6}$$

Creating a 3D Model and Mesh

The composite pipe design to be pressure tested was designed in Solidworks program with a length of 500 mm according to ISO 1167 standards. Pipe and pipe dimensions of 125 mm outer diameter, which are used as a standard in natural gas infrastructure works, are taken as reference.

The equation used in ISO 1167 standards is used to calculate the test pressure of the pipe to be used under 19 bar pressure.

$$p = 10 \times \sigma \frac{2xe}{d - e} \tag{7}$$

$$p = 10 \times 19 \frac{2 \times 11,2}{125 - 11,2} = 37.5 \text{ bar}$$

There are 108656 nodes and 20928 elements in the analysis model.

Table 8. Densities of 15% reinforced composite materials.

	Density of matrix material (gr/cm ³)	Density of fiber material (gr/cm ³)	Total density (gr/cm ³)
PP+%15 AF	0.90	1.44	0.98
PE+%15 AF	0.95	1.44	1.02
8	31.92	30.081258	42.9142

Table 9. Pipe dimensions.

outer diameter (mm)	inner diameter (mm)	wall thickness (mm)
125	102.6	11.2

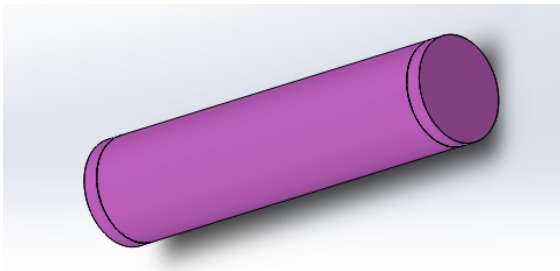


Figure 10. Composite pipe design.

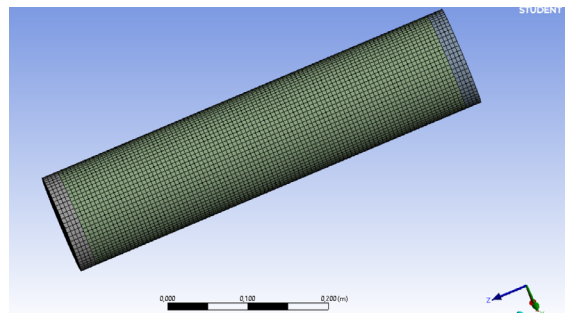


Figure 11. Analysis model of composite pipe.

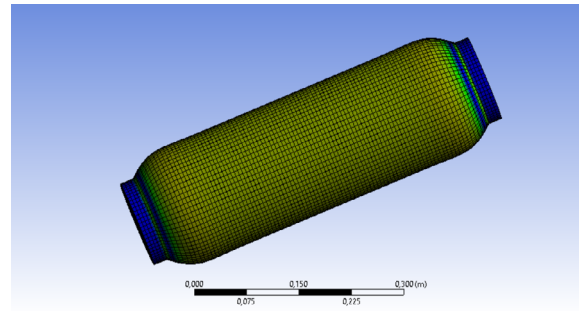
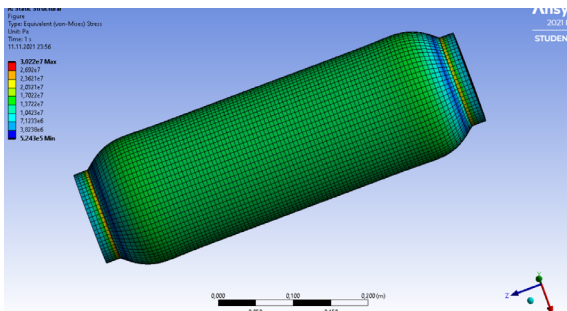


Figure 12. Finite Element Analysis Results of PP+%15 AF a)Equivalent Stress, b)Safety Factor.

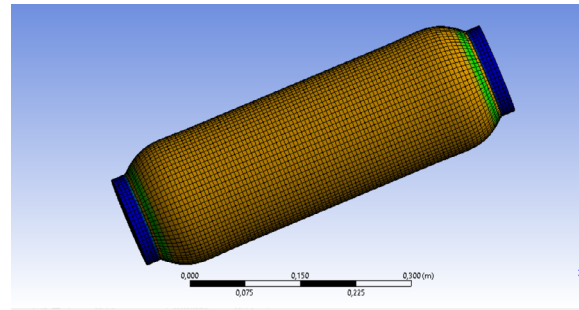
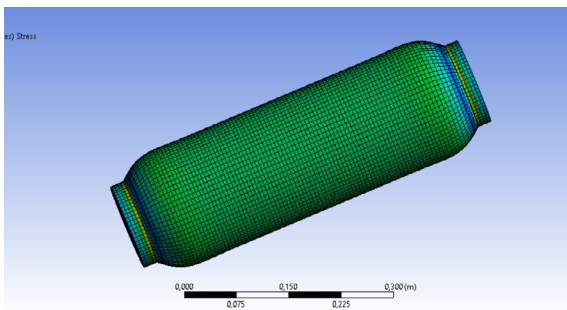


Figure 13. Finite Element Analysis Results of PE+%15 AF a)Equivalent Stress, b)Safety Factor.

Defining Boundary Conditions

The two ends of the composite pipe to be tested were closed with a steel cap and the mechanical behavior of the material was examined at 37.5 bar pressure.

Finite Element Analysis Results

When Figure 12-13 is examined, it is seen that the factor of safety of PP+15%AF is 2.44, and the factor of safety of PE+15%AF is 1.36.

CONCLUSION

1-It was concluded that the type of reinforcement material, the degree of adhesion between the matrix and the interface, the fiber percentage and its orientation in the matrix affect the mechanical properties of the composite.

2-It was observed that the mechanical values of the composites increased with the increase in the reinforcement fiber ratio. The fiber yield decreased due to the withdrawal of aramid fibers from the matrix and the deformations around the fiber.

3-Aramid fiber showed higher performance over PE matrix composite. The surface energy of the matrix affected the efficiency of the composites formed with the fiber. Surface energy of the PP matrix is lower than that of the PE matrix, the composite with PP matrix performed better.

4-According to the results of ANOVA analysis, it is seen that the percentages of effect of matrix and fiber additive ratios on the mechanical properties of composite materials are different.

5-The safety coefficient of the pipe designed from PP+15% AF composite material is 2.45. Therefore, the safest composite material was found to be PP+15% AF.

References

1. KK. Kar (Ed.), *Composite Materials: Processing, Applications, Characterizations*, Springer Berlin, Germany, 2016.
2. S.Y. Fu, B. Lauke, and E. Mader, Fracture resistance of unfilled and calcite-particle filled ABS composites reinforced by short glass fiber (SGF) under impact load. *Composites Part A*, 29 (1998) 631–41
3. T. Harmia, J. Hartikainen and M. Lindner, Long Fiber-Reinforced Thermoplastic Composites in Automotive Applications. *Polymer Composites*, (2005) 255–262.
4. T.P. Sathishkumar, S. Satheeshkumar, and J. Naveen, Glass fiber-reinforced polymer composites – a review. *Reinforced Plastics and Composites*, 33 (2014) 1258-1275
5. D.S. Choudhari and V.J. Kakhandki, Comprehensive study and analysis of mechanical properties of chopped carbon fibre reinforced nylon 66 composite materials. *Materials Today: Proceedings*. (2020) Doi: 10.1016/j.matpr.2020.10.828.
6. B. M. İçten, R. Karakuzu, and M. E. Toygar, Failure analysis of woven kevlar fiber reinforced epoxy composites pinned joints. *Composite Structures*, 73(4) (2006) 443–450 doi: 10.1016/j.compstruct.2005.02.016.
7. B.W. Imes, *Glass-Polymer Composite Pipes and Joints: Manufacturing, Testing, and Characterization* (Doctoral thesis, West Virginia University, Morgantown) Accessed from database ProQuest Dissertations and Theses. (2018) (UMI No. 10793813)
8. H. Chen, J. Wang, A. Ni, A. Ding, Z. Sun, and X. Han, Effect of novel intumescent flame retardant on mechanical and flame retardant properties of continuous glass fiber reinforced polypropylene composites. *Composite Structures*, 203 (2018) 894–902
9. P. K. Mallick, 2.18 Particulate Filled and Short Fiber Reinforced Polymer Composites. *Comprehensive Composite Materials II*. (2018) 360–400. doi:10.1016/b978-0-12-803581-8.03837-6
10. H.-Q. Xie, S. Zhang and D. Xie, An efficient way to improve the mechanical properties of polypropylene/short glass fiber composites. *Applied Polymer Science*, 96(4) (2005) 1414–1420 doi:10.1002/app.21575
11. S. Panthapulakkal and M. Sain, Injection-molded short hemp fiber/glass fiber-reinforced polypropylene hybrid composites—Mechanical, water absorption and thermal properties. *Applied Polymer Science*, 103(4) (2006) 2432–2441 doi:10.1002/app.25486.
12. J. O. Akindoyo, M. D. H. Beg, S. Ghazali, H. P. Heim, M. Feldmann, and M. Mariatti Simultaneous impact modified and chain extended glass fiber reinforced poly(lactic acid) composites: Mechanical, thermal, crystallization, and dynamic mechanical performance. *Applied Polymer Science*, (2020) 49752. Doi:10.1002/app.49752.
13. R. Day, K. Hewson and P. Lovell, Surface modification and its effect on the interfacial properties of model aramid-fibre/epoxy composites. *Composites Science and Technology*, 62(2) (2002) 153–166. doi:10.1016/s0266-3538(01)00135-x.
14. G. Qi, B. Zhang and S. Du, Assessment of F-III and F-12 aramid fiber/epoxy interfacial adhesions based on fiber bundle specimens. *Composites Part A: Applied Science and Manufacturing*, 112 (2018) 549–557. doi: 10.1016/j.compositesa.2018.06.001.
15. S. L.Crabtree, M. A. Spalding and C. L. Pavlicek, Single-screw extruder zone temperature selection for optimized performance. *ANTEC*, (2008) 1410-1415.
16. H. M. Da Costa, V. D. Ramos and M. G. Oliveira, Degradation of polypropylene (PP) during multiple extrusions: Thermal analysis, mechanical properties and analysis of variance. *Polymer Testing*, 26(5), (2007) 676–684. doi: 10.1016/j.polymeresting.2007.04.003.
17. B. Alişer, S.Yıldız, E. Arıcı and O. Keleştemur, Analysis of Sulfate Resistance of Cement Mortars Containing Glass Fiber and Marble Dust by Using Taguchi Method. 2nd International Sustainable Buildings Symposium, (2015) 117-122.
18. M. Savaşkan, Y. Taptık and M. Ürgen, Performance Optimization of Drill Bits Using Design of Experiments. *İtÜdergisi/d mühendislik*, 3 (6) (2004) 117-128.
19. B. Özçelik, and A. Özbay, Determination of Effect On the Mechanical Properties of Polypropylene Product of Molding Materials Using Taguchi Method. *Engineering and Natural Sciences*, Sigma 29, (2011) 231-243.
20. T. Fu, B. Haworth and L. Mascia, Analysis of process parameters related to the single-screw extrusion of recycled polypropylene blends by using design of experiments. *Plastic Film & Sheeting*, 33(2), (2016) 168–190. doi:10.1177/8756087916649006
21. N. Ravi Kumar, P. Srikant, C. Ranga Rao and K. Meera Saheb, Statistical analysis of mechanical properties of vakka fiber reinforced polypropylene composites using Taguchi method. *Materials Today: Proceedings*, 4(2), (2017) 3361–3370. Doi: 10.1016/j.matpr.2017.02.224.
22. G. Ozkoc, G. Bayram and E. Bayramli, Short glass fiber reinforced ABS and ABS/PA6 composites: Processing and characterization. *Polymer Composites*, 26(6), (2005) 745–755. doi:10.1002/pc.20144.
23. D. W. Callister, G. D. Rethwisch, *Materials Science and Engineering*, WILEY, New York, 2015.
24. A. Ari, A. Bayram, M. Karahan, Comparison of the mechanical properties of chopped glass , carbon , and aramid fiber reinforced polypropylene. *Polymers and Polymer Composites*, 30 (2022) 1–13 <https://doi.org/10.1177/09673911221098570>
25. A. Ghanbari, N.S. Jalili, S.A. Haddadi, M. Arjmand and M. Nofar, Mechanical properties of extruded glass fiber reinforced thermoplastic polyolefin composites. *Polymer Composites*, 41(9), (2020) 3748-3757. <https://doi.org/10.1002/pc.25672>.
26. S. Kumar and S. Balachander, Studying the effect of reinforcement parameters on the mechanical properties of natural fibre-woven composites by Taguchi method. *Industrial Textiles*, (2019) 1-16 doi:10.1177/1528083718823292.
27. C. Lu, J. Wang, X. Lu, T. Zheng, Y. Liu, X. Wang and D. Seveno, Wettability and interfacial properties of carbon fiber and poly (ether ether ketone) fiber hybrid composite. *ACS Applied Materials and Interfaces*. (2019) doi:10.1021/acsami.9b09735
28. F. Fenouillot, P. Cassagnau and J.-C. Majesté, Uneven distribution of nanoparticles in immiscible fluids: Morphology development in polymer blends. *Polymer*, 50(6), (2009) 1333–1350. doi:10.1016/j.polymer.2008.12.029
29. S. Somashekhar, G. C. Shanthakumar and M. Nagamadhu, Influence of Fiber content and screw speed on the Mechanical characterization of Jute fiber reinforced Polypropylene composite using Taguchi Method. *Materials Today: Proceedings*, 24, (2020) 2366–2374. doi:10.1016/j.matpr.2020.03.766.ca